

Supporting Information

Probing the Mechanism for Graphene Nanoribbon Formation

on Gold Surfaces through X-ray Spectroscopy

Arunabh Batra¹, Dean Cvetko^{2,3}, Gregor Kladnik^{2,3}, Olgun Adak¹, Claudia Cardoso⁴,
Andrea Ferretti⁴, Deborah Prezzi⁴, Elisa Molinari^{4,5},
Alberto Morgante^{*,3,6}, Latha Venkataraman^{*,1}

¹ *Department of Applied Physics and Applied Mathematics,
Columbia University, New York, NY, USA*

² *Department of Physics, University of Ljubljana, Ljubljana, Slovenia*

³ *CNR-IOM Laboratorio Nazionale TASC, Basovizza Trieste, Italy*

⁴ *Istituto Nanoscienze, Consiglio Nazionale delle Ricerche, Modena, Italy*

⁵ *Department of Physics, Mathematics and Informatics, University of Modena and
Reggio Emilia, Modena, Italy*

⁶ *Department of Physics, University of Trieste, Trieste, Italy*

* Corresponding Authors: (LV) lv2117@columbia.edu; (AM) morgante@iom.cnr.it

Contents:

- 1. Theoretical Details**
- 2. Sample Preparation**
- 3. Additional Data**
- 4. References**

1. Details of Theoretical Calculations

We perform density functional theory (DFT) based theoretical calculations to understand the electronic structure of the gold surface state with and without a graphene nano ribbons over layer. Simulations were performed within the local density approximation (LDA) for the exchange-correlation potential, using a plane-wave basis set and ultrasoft pseudopotentials, as implemented in the Quantum-ESPRESSO package¹. The kinetic energy cutoff for the wave functions (charge density) was set to 25 (300) Ry. We considered both the pristine Au(111) surface and Au(111) with the adsorbed GNR. The surfaces were modeled using a five-layer slab of Au(111); a $3 \times 4\sqrt{3}$ supercell was employed to accommodate the GNR. Slabs were passivated with H on one side to inhibit interaction between Au(111) surface states resulting from the finite thickness of the slab. Moreover, slab replicas were separated by a vacuum region of 12 Å in order avoid spurious interactions. The in-plane lattice parameter was set to the optimized parameter for bulk Au (4.05 Å), and the atomic positions within the cell were fully optimized, with a force threshold of 0.013 eV/Å.

When studying a pristine Au(111) slab, the finite width of the slab model leads to a artificial interaction of the states located on the two surfaces, resulting in two non-degenerate surface states. Eventually, the energies of these states converge to the same value when the number of layers is increased. The interaction between these states can be prevented by passivating one of the surfaces with H atoms, thereby removing one of the two surface states. This allows one to model the Au slab with a smaller number of atomic layers. The convergence with respect to the number of layers was verified both for H passivated and non-passivated slabs, as shown in Figure S7. When considering the hydrogenated Au(111) slab, the onset of the surface states at Γ is found to be converged with 5 layers.

2. Sample Preparation

The Au substrates are first cleaned by repeated cycles of Ar sputtering and annealing to 800K. Helium atom scattering (HAS) with a He beam energy of 19 meV is then used to confirm the characteristic herringbone reconstruction of Au(111) or the 1x2 missing-row

reconstruction of the Au(110) substrate. XPS measurements of the Au are made to ensure no contamination on the sample. The operational pressure for the measurement chamber is maintained at 10^{-11} mbar and the sample preparation chamber at 10^{-10} mbar. DBBA from AOKBIO (98+% purity) is deposited on this substrate from a quartz Knudsen-type cell in line-of-sight with the sample preparation chamber. For monolayer deposition, the Au substrate is maintained at room temperature, and the Knudsen cell is heated to 490K. The molecule is deposited at a chamber pressure of 10^{-8} mbar with a typical rates of 2 Å/min. DBBA deposition and coverage is controlled by Helium (He) specular reflectivity and XPS. As molecules cover the Au crystalline surface the He specular intensity attenuates strongly (Figure S2), and eventually disappears in the diffuse background as the Au surface is covered. Due to larger-than-geometrical cross section for diffuse He scattering, the HAS signal disappears well before the full molecular monolayer fully covers the substrate. Formation of any further layers of molecules beyond monolayer may be also witnessed by the shift of XPS peaks to higher binding energies, due to reduced screening of the core hole by the metal substrate.—HAS measurements were carried out at the HASPES beamline at the Elettra Synchrotron, Trieste, Italy. Details can be found in previously published work.²

3. Additional Data

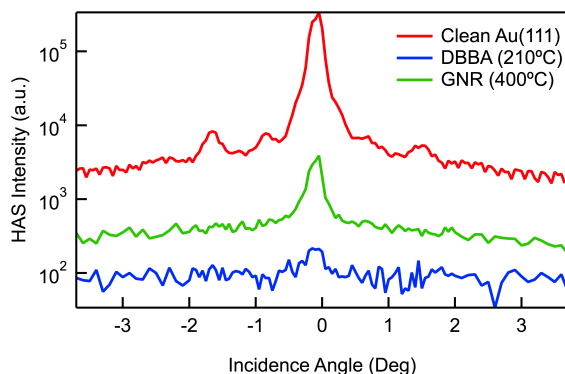


Figure S1: HAS intensity as a function of incident beam angle. Clean Au(111) (red) shows a strong peak at the specular angle (0). DBBA is deposited with the sample temperature at 210 C, resulting in the diminishment of the specular peak (blue) due to a disordered layer. Heating this film to 400 C (green) shows that HAS signal partly recovers, signifying an increasingly ordered surface commensurate with polymerization and GNR formation.

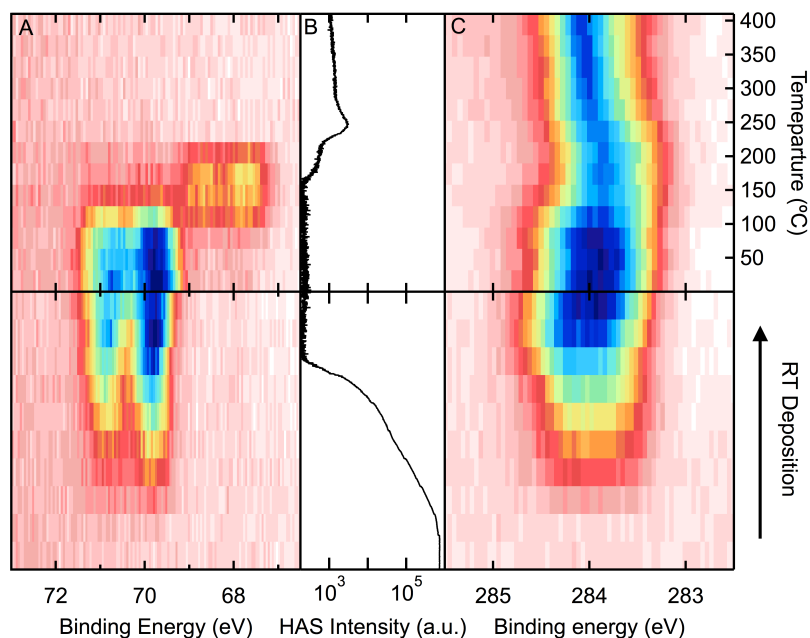


Figure S2: Simultaneous measurement of HAS Specular Reflectivity and XPS signal as a function of DBBA deposition time (lower panel) and annealing temperature on Au(111) (upper panel). A) Br 3d XPS signal. B) HAS Specular intensity. C) C1s XPS signal. The HAS intensity is lowest after molecule deposition at RT and increases as the substrate is annealed.

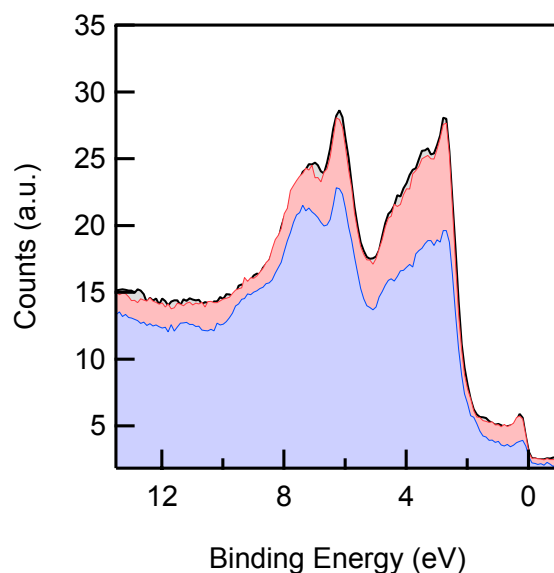


Figure S3: UV photoemission (UPS) spectrum for GNR (black, solid). Additional deposition at 100C (blue) results in a diminished gold signal, and molecular resonances appearing. On heating above 200 C (red), the film recovers original UPS spectrum, showing that the original GNR film was saturated and inert.

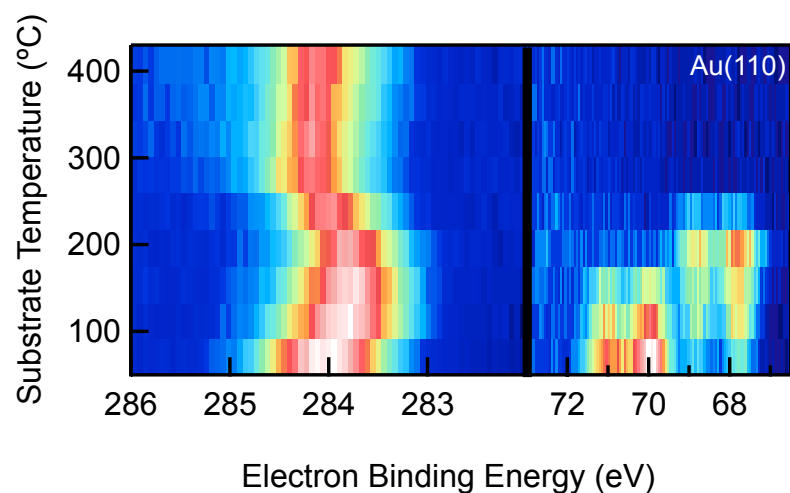


Figure S4: Temperature dependent XPS for C 1s (left panel) and Br 3d (right panel) for DBBA/Au(110). The overall evolution of the XPS signal is similar to that of DBBA/Au(111) presented in the main text, with the molecular de-bromination starting already at 50 C.

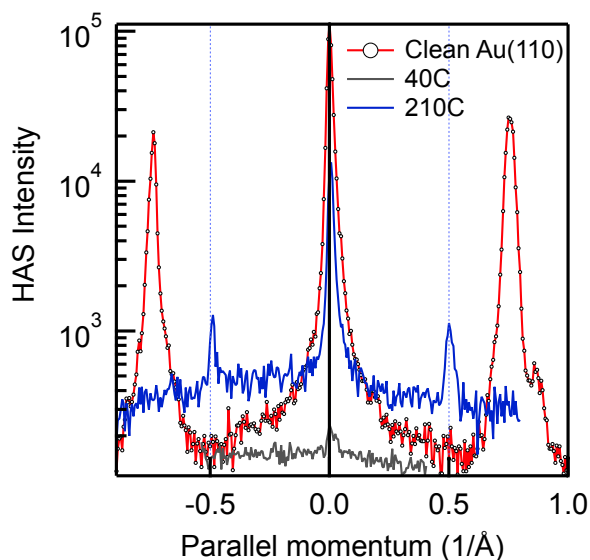


Figure S5: Helium Atom Scattering (HAS) on DBBA/Au(110). HAS Intensity as a function of incident beam angle for different film conditions. Clean Au(110) (red) shows the characteristic spectrum of the 1x2 missing row reconstruction. A monolayer of DBBA is deposited at RT, resulting in the diminishment of the specular peak (black) due to disordered adsorption of the molecule. Heating this film to 210 C (blue) shows that the signal recovers but with a 1x3 reconstruction, suggesting that molecule-metal interaction changes the surface reconstruction.

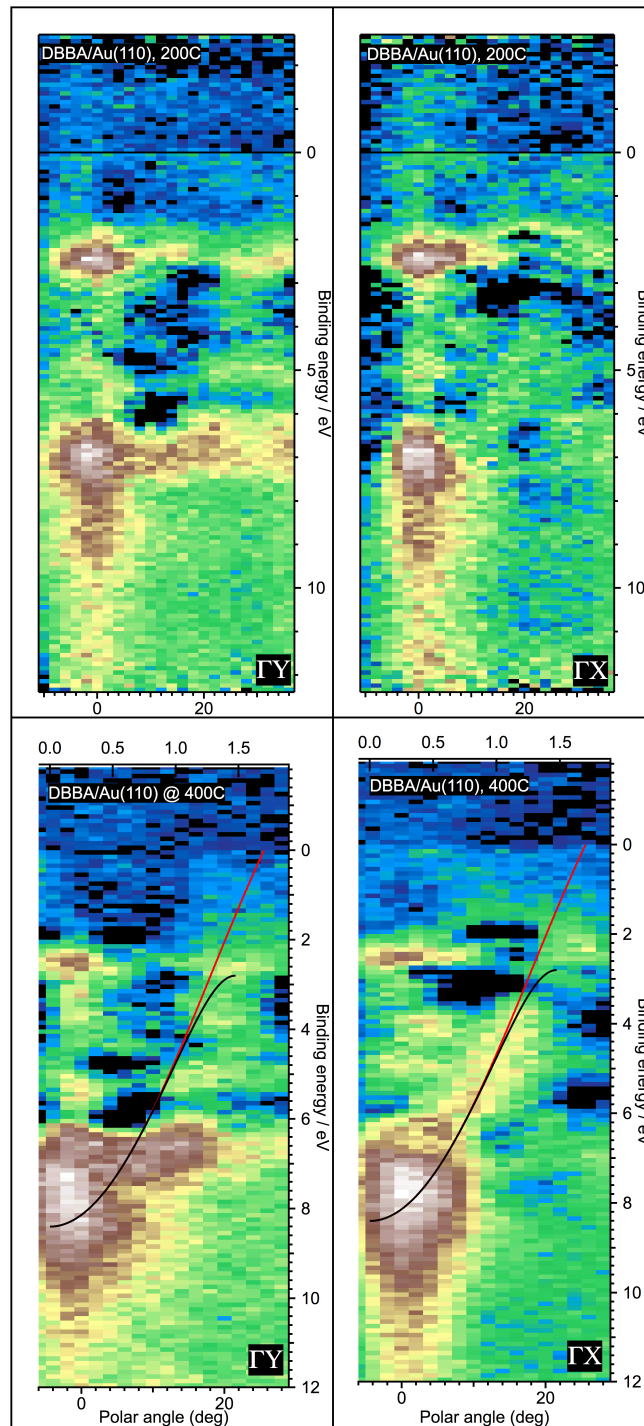


Figure S6: ARUPS for DBBA/Au(110) (a) at 200 C along the ΓY direction of the substrate, (b) at 200 C along the ΓX direction of the substrate, (c) at 400 C along the ΓY direction of the substrate and (d) at 400 C along the ΓX direction of the substrate. A band-like dispersion is seen at 400 C in (d) but not in (c) indicating that the GNRs are aligned along the $[1\bar{1}0]$ direction of the Au(110) surface. Graphene-like band is overlaid in (c) and (d) as solid black (ΓM) and red (ΓK) curves.

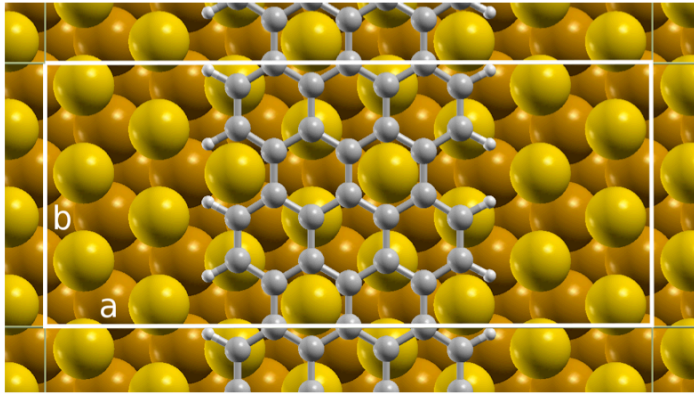


Figure S7: Unit cell of the GNR + Au(111) surface system used in the calculations. The cell parameters of the unit cell in surface plane are $a=19.84 \text{ \AA}$ and $b=8.59 \text{ \AA}$. The surfaces were modeled using a five-layer slab of Au(111). Slabs were passivated with H on one side. Slab replicas were separated by a vacuum region of 12 \AA .

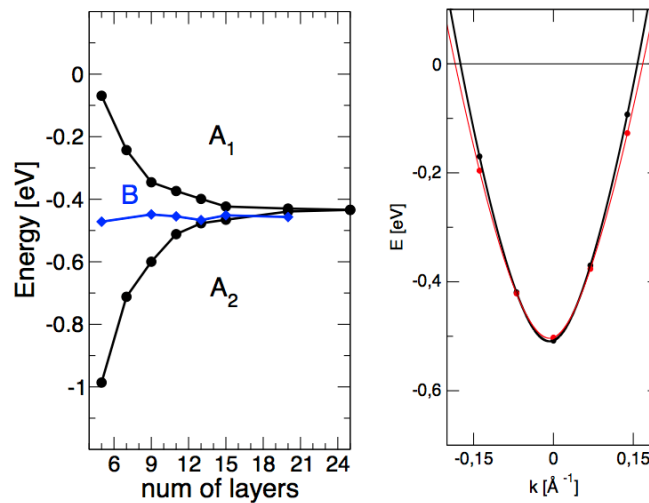


Figure S8. (Left) Energy of the bottom of the surface band computed for slabs with different number of Au layers, both for non-hydrogenated (A_1 and A_2) and hydrogenated (B) slabs. All calculations were performed at the LDA level. (Right) Au surface band dispersion for 5 (red) and 20 (black) Au layers. The black trace is shifted vertically (by 0.02 eV) to highlight the difference between the two at E_F .

References:

1. P. Giannozzi, et al, *J. Phys.:Cond. Mat.*, 2009, **21**, 395502.
2. D. Cvetko, A. Lausi, A. Morgante, F. Tommasini, K. C. Prince and M. Sastry, *Measurement Science & Technology*, 1992, **3**, 997-1000.